Plant Soil (2009) 319:67–84
DOI 10.1007/s11104-008-9850-7

REGULAR ARTICLE

Sediment deposition and soil nutrient heterogeneity in two desert grassland ecosystems, southern New Mexico

Junran Li · Gregory S. Okin · Lorelei J. Alvarez · Howard E. Epstein

Received: 17 July 2008 / Accepted: 25 November 2008 / Published online: 10 December 2008

Abstract The role of wind in changing the spatial heterogeneity of soil resources in erosion-dominated semiarid ecosystems is well known. Yet the effect of windblown sediment deposition on soil nutrient distribution and ecosystem dynamics at local and landscape scales has received little attention. We examined the effects of enhanced sediment deposition on the spatial distribution of soil nutrients at the Jornada Experimental Range, southern New Mexico. Enhanced sediment deposition was obtained as a result of grass cover reduction in the upwind portion of the experiment in two sites co-dominated by mesquite and one of two grass species with different morphologies. The spatial characteristics of soil available nitrogen (including ammonium, nitrite, and nitrate), phosphate, potassium, and calcium were quantified using a variety of traditional and geostatistical analyses. Our results showed that enhanced deposition led to considerable reduction in both mean soil nutrient concentrations and coefficients of variation over a two-year period (2004–2006). Given the observed increase in the scale of spatial dependence for available nitrogen, but not for potassium, phosphate, and calcium following enhanced sediment deposition, we suggest that soil available nitrogen may be particularly responsive to increased aeolian activities due to livestock grazing and other anthropogenic activities that remove vegetation. Our study further suggests that soil particles deposited in the downwind area may be "nutrient-imbalanced." Specifically, the lower-than-normal available nitrogen concentrations in the wind-deposited soils may inhibit the growth of grasses and the germination of seeds. For wind-erodible ecosystems found in southern New Mexico, structures of *Bouteloua*-dominated communities may be particularly susceptible to change under enhanced soil erosion conditions.

Keywords Aeolian processes · Available nitrogen · Sediment deposition · Spatial heterogeneity · Geostatistics · Ecosystem dynamics

Responsible Editor: Elizabeth (Liz) A. Stockdale.

J. Li · L. J. Alvarez · H. E. Epstein
Department of Environmental Sciences,
University of Virginia,
Clark Hall, 291 McCormick Rd.,
Charlottesville, VA 22904-4123, USA

G. S. Okin
Department of Geography, University of California,
1255 Bunche Hall, Box 951524,
Los Angeles, CA 90095, USA

Present address:
J. Li (✉)
Department of Biological and Environmental Engineering,
Soil and Water Lab, Cornell University,
Riley-Robb Hall,
Ithaca, NY 14853, USA
e-mail: jl2428@cornell.edu

Introduction

In many arid and semiarid ecosystems, aeolian processes are principal agents of topographic change, land degradation and ecosystem dynamics (Leys and McTainsh 1996; Ayoub 1998; Barth 1999; Okin and Gillette 2001; Li et al. 2007). Aeolian processes consist of three components: erosion, transport, and the subsequent deposition of particles. Erosional loss of soil from land surfaces can dramatically change topography, soil properties, and plant productivity (Larney et al. 1998; Gillette and Monger 2006; Li et al. 2008). The long-distance transport of dust particles affects public health due to soil-borne contaminants and degraded air quality (Griffin et al. 2001; Reheis 2006), and the deposition of dust is thought to play a major role in ocean fertilization, CO_2 uptake, terrestrial soil formation, and nutrient cycling (Chadwick et al. 1999; Piketh et al. 2000; Reynolds et al. 2001). At local and landscape scales (10 s of m–10 s of km), dust emitted from one area may have significant impacts on the nutrient status of downwind soils, since soil organic matter and nutrients such as N and P tend to be concentrated on dust particles (Leys and McTainsh 1994; Okin et al. 2004; Li et al. 2007). However, most of the research on the effects of dust deposition has focused on global scales using mathematical modeling, remote sensing, or records of long-term deposition in soils (e.g., Chadwick et al. 1999; Reynolds et al. 2001; Reheis 2006; Neff et al. 2008). To our knowledge, no study to date has experimentally studied the effects of enhanced aeolian deposition on soil nutrient distribution at local and landscape scales.

Our recent research at the Jornada Experimental Range in southern New Mexico indicates that aeolian processes are tightly linked to the spatial distribution of soil resources at both plant-interspace (0.1–10 m) and patch scales (10–100 m) (Peters et al. 2006). For instance, in erosion-dominated plots, wind has been shown to deplete 25% of soil organic carbon (SOC) and soil total nitrogen (TN) in three windy seasons (Li et al. 2007). In a plot area of 5 m×10 m, geostatistical analyses have revealed that soil resource heterogeneity, especially for SOC and TN, increases significantly as a result of enhanced wind erosion (Li et al. 2008). Studies have also identified the deposition of fine-grained windblown materials under shrubs as one of the factors responsible for the conversion of grasslands to desert shrublands occurring in southern New Mexico over the past 150 years (Coppinger et al. 1991; Schlesinger et al. 1996).

The results of enhanced aeolian processes on ecosystem dynamics have been demonstrated by an all-plant-removal "scraped site" implemented in 1991 for an experiment aimed at measuring dust flux from loamy sand soils at the Jornada Experimental Range (Okin et al. 2006). After more than a decade, the site itself and the area directly downwind have undergone major changes in soil nutrient status and plant community composition. Up to 82% of N and 62% of plant available P in the surface soil of the scraped site have been depleted, and the deposition initiated conversion of the downwind grassland to a shrubland (Okin et al. 2001). However, the scraped site was not a well-monitored, replicated experiment. New experiments are required to provide quantitative details on the impact of aeolian processes on ecosystem dynamics, such as sediment flux and changes of soil nutrient variation in both wind-eroded and downwind deposition areas. In previous studies, a unique field-based, erosion-enhancement experiment was used to investigate soil nutrient depletion and spatial variation in upwind erosion-dominated treatment plots (Li et al. 2007, 2008). In this study, we report results on sediment deposition and changes to the spatial distribution of soil nutrients in the deposition-dominated downwind of the treatment plots. Li et al. (2007) further suggest that plots with low vegetation cover displayed enhanced soil mass and nutrient flux. This material, when transported downwind will tend to collect beneath plant canopies rather than in bare interspaces, thus, changing the spatial heterogeneity of soil resources. This hypothesis was evaluated using conventional and geostatistical analysis of soil nutrient concentrations of soil samples through deposition-enhanced and control plots.

Methods

Site description

We conducted the study at the USDA-ARS Jornada Experimental Range (JER), located in the northern Chihuahuan Desert (Fig. 1). The JER was established in 1912 and now is part of the National Science Foundation's Long Term Ecological Research (LTER)

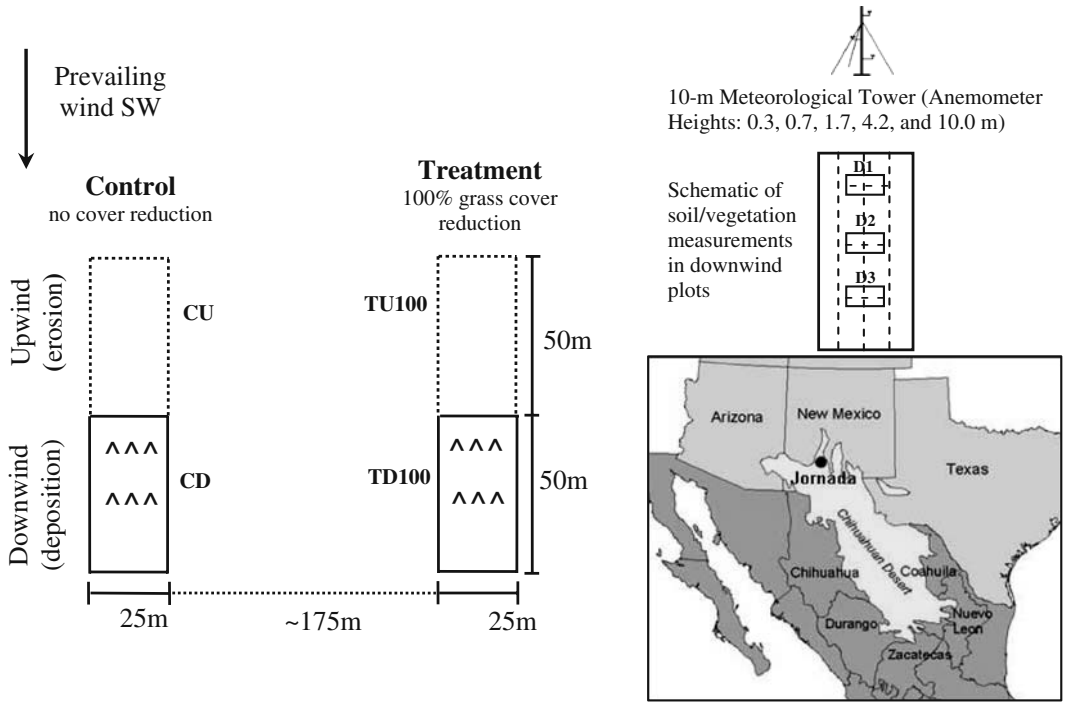

Fig. 1 Location of the study sites (Jornada LTER, lower-right corner) and the experimental layout in the field. Dashed squares represent upwind erodible vegetation cover reduction plots. Solid squares represent downwind depositional plots where no vegetation cover was reduced. "^" represents BSNE sediment samplers. The right-most figure shows more detailed layout of sampling locations and plant investigation transects in downwind plots. Soil sampling was conducted in the D1 subplots, BSNEs were installed in both D1 and D2 subplots, and erosion bridges (represented by "-") were installed in all D1, D2 and D3 subplots. Three 50-m line-intercept transects were set up for plant community monitoring (denoted by dashed line). The field site was fence-protected

network. Long-term mean annual temperature is 15.6°C, and mean maximum temperatures are 36°C and 13°C in June (warmest month) and January (coldest month), respectively. Mean annual precipitation (P) (1915–2002) and potential evapotranspiration (PET) recorded at the JER headquarters (32 37′ N, 106 44′ W) are 24.7 cm and 230 cm yr^{-1}, respectively, yielding a P/PET value of just greater than 0.1. Soils at the JER are quite complex, but sands and sandy loams are generally widespread (Bulloch and Neher 1977).

Two field sites were set up in Pasture 11 of the JER (Table 1). Site 1 and site 2 were set up in March and July 2004, respectively. These sites have sparse vegetation cover and are typical grass/shrub mixed communities at the JER. Although both sites have similar topography and soils, different plant species dominate each. Site 1 is dominated by *Sporobolus* spp. grasses (primarily *S. flexuosus* and *S. contractus*) and mesquites, and is hereafter referred to as the *Sporobolus*-mesquite (SM) site. Site 2 is dominated by *Bouteloua eriopoda* and mesquites, and is hereafter referred to as the *Bouteloua*-mesquite (BM) site. Our research sites are susceptible to erosive winds in the spring time, which frequently exceed 25 m s^{-1} (Helm and Breed 1999). Soil A-horizon depth at both study sites was >10 cm to avoid complete excavation by deflation during the experiment. In addition, both sites are underlain by a petrocalcic horizon >1 m depth, with parent material of wind-reworked fluvial sands up to 100 m in depth (Okin and Gillette 2001).

Experimental design and sampling method

At each site, two 25 m×50 m rectangle plots, including one wind-erosion enhanced plot and one control plot, are aligned with the 50 m sides parallel to prevailing winds (upwind plots); and two 25 m×50 m plots are located immediately downwind of the upwind plots (Fig. 1). Observations at the JER scraped site suggest that 50 m fetch was adequate to allow significant aeolian transport (Gillette and Chen 2001). Enhanced dust and sand deposition in the downwind plots was

Table 1 Environmental characteristics of the study sites before the initiation of enhanced sediment deposition

Characteristics	*Sporobolus*-mesquite site (SM site)		*Bouteloua*-mesquite site (BM site)	
	TD100	Control	TD100	Control
Plant cover (%)				
Total cover	23	25	22	27
Grass	4	9	12	9
Prosopis	6	5	6	10
Gutierrezia	1	<1	1	2
Forb	12	10	3	6
Dominant species	*Sporobolus spp., Prosopis glandulosa*		*Bouteloua eriopoda, Prosopis glandulosa*	
Shrub diameter (m, means ±1SD)	1.62±0.28	1.89±1.00	1.26±0.86	1.07±0.72
Surface Soil				
Sand (%)	98	98	95	94
Silt and clay (%)	2	2	5	6
texture	Sand		Sand	
Caliche exposure	No		No	
Biological crust	Occasional		Frequently seen	
Geomorphology				
Slope (%)	<1		<1	
Parent material	Wind-reworked fluvial sands		Wind-reworked fluvial sands	
Mesquite dunes	Small-no		No	

achieved by grass cover reduction in the upwind area. Detailed set up and grass cover reduction procedures in the upwind plots were described by Li et al. (2007). In short, in the 100% grass cover reduction plot (simplified as TU100), all grasses, perennial semi-shrubs such as *Gutierrezia sarothrae*, and perennial forbs were removed (hereafter referred to as "grass cover reduction" only). Shrub cover was low in both sites at the beginning of the experiment, and shrubs were not removed in the upwind area. No vegetation cover was reduced in the control plots nor in the downwind areas. Enhanced sediment deposition in the downwind plots was maintained by keeping the appropriate reduced cover on the upwind plots during the entire experimental period.

In the downwind plots, sediment flux was monitored using Big Spring Number Eight (BSNE, Custom Products, Big Springs, Texas) sediment samplers installed at two distances from the upwind-downwind boundary (D1 and D2 subplots, Fig. 1). These sediment samplers and their calibration were described by Fryrear (1986). The BSNE trap is a sheet metal slot-type collector consisting of a rectangular inlet area of about 20 mm×50 mm. The BSNE samplers maintain 90% efficiency (ratio of collector flux to actual flux) for sand particles (50 μm to 2 mm diameter) at various wind speed (Shao et al. 1993). Three stems, each with four BSNE traps and wind vanes (so the traps orient into the wind), were placed approximately 3-4 m apart along the center of each 5 m×10 m subplot (D1 and D2). The traps on each stem were situated at 0.1, 0.3, 0.6 and 1.2 m above the ground. Placement of BSNE stems directly downwind of shrubs was avoided. Windblown sediment samples were collected twice per year in early March (non-windy season, sampling period from previous July to March) and middle July (windy-season, sampling period from March-July) from 2004 to 2006. A total of 480 and 384 sediment samples were obtained in the SM site and BM site, respectively.

In addition, soil deflation/aggradation in the downwind area was monitored by "erosion bridges," a method used by Gillette and Chen (2001) to measure differential soil surface height. The erosion bridges were constructed from rebar and bent to the shape of a soccer goal post, and they were pounded into the soil 20–30 cm in depth. In each downwind plot, five erosion bridges were installed about 1-2 m apart along the center of each 5 m×10 m subplots (D1, D2, and D3, Fig. 1). Similar to the BSNEs, placement of erosion bridges within or directly downwind of shrubs was avoided. Heights of the erosion bridges (distance

from the soil surface to the top of the erosion bridge) were carefully recorded once per year in July from 2004 to 2006, except for the BM site, where erosion bridges were first monitored in March 2004. A total of 60 erosion bridges were installed and 210 measurements were obtained.

To study sediment deposition and soil nutrient heterogeneity, fifty soil samples of 2.5 cm diameter from the top 5 cm of soil were taken in the D1 subplots of TD100 (downwind of TU100) and the downwind control plot in July 2004, and again after two windy seasons in July 2006 (Fig. 1). A total of 400 soil samples were collected and analyzed. Large debris was removed from the soil surface to facilitate sampling, but no effort was made to clear the top of the mineral soil prior to sampling. Soil samples were randomly distributed without regard to plant locations and a different set of sampling coordinates were adopted each year. The relative locations of each soil sample within the 5 m×10 m subplots were precisely identified for geostatistical analysis.

In both study sites, a 10 m meteorological tower was installed 60 m upwind of the treatment area with five anemometers arranged at heights of 0.3, 0.7, 1.7, 4.5, and 10.0 m (Fig. 1). Wind speed and directions were recorded every 5 min. Precipitation during the whole experimental period was recorded using a tipping bucket rain gage installed approximately 100 m upwind of the treatment area. Plant cover and community composition on each plot were monitored by three 50 m line-intercept transects in spring (March) and summer (July) each year during the experimental period. Plant cover was calculated by adding the lengths of each plant species along the transect and dividing by the total length of the transect. In addition, for each plant in the soil sampling subplots (D1, Fig. 1), its location, height, and basal area were recorded in July 2004 and July 2007 using a Trimble 3600 Total Station System to examine effects of enhanced deposition on plant presence and community composition.

Laboratory analysis

In the laboratory, each BSNE sediment sample was weighed to 0.001 g to yield sediment flux. Each soil sample was air-dried and sieved through a 2 mm screen to remove gravels, roots, and debris. Water-extractable anions of soil samples such as Cl^-, NO_2^-, NO_3^-, SO_4^{2-}, and PO_4^{3-} were analyzed on a Dionex ICS-2000 ion chromatograph (IC) following the method of Schlesinger et al. (1996). Exchangeable cations, such as Na^+, K^+, Mg^{2+}, and Ca^{2+} were analyzed by the $BaCl_2$ extraction method according to Hendershot and Duquette (1986). Extracts were analyzed on a Dionex ICS-2000 IC with an Ion Pac CS 12A cation exchange column. The studies by Horn et al. (1982) and Gillman et al. (1983) indicate that the $BaCl_2$ extraction method gives comparable results to procedures using $NH_4C_2H_3O_2$ and KCl extractions for K^+ and non-K^+ cations, respectively.

For this study, NH_4^+ was also extracted with the 0.1 mol L^{-1} $BaCl_2$ solution. Li et al. (2008) showed that NH_4^+ measured from a 2 mol L^{-1} KCl extract was highly correlated (r=0.96) to NH_4^+ in the 0.1 mol L^{-1} $BaCl_2$ extract. This strong correlation suggests that the $BaCl_2$ extraction should be a dependable index of NH_4^+ availability. Additionally, the $BaCl_2$ extraction method allowed us to analyze all cations simultaneously on the IC since the chromatogram peak of Ba^{2+} appears well behind the cations of interest. All soil data are reported as milligrams per kilogram of soil. We report the sum of NO_2^-, NO_3^- and NH_4^+ as the index of total available N (N_{avail}).

Calculations and statistical analyses

Wind erosion rates, represented by horizontal sediment flux, were calculated according to Gillette and Pitchford (2004) and presented formally in Li et al. (2007). Briefly, the mass of airborne particles collected by a BSNE trap was divided by the inlet area and the time of the collection to yield time-averaged horizontal flux $Q(z)$ (units of g m^{-2} day^{-1}), where z is the height of BSNE traps above ground. Values of $Q(z)$ were then fit to an exponential function, and integrating this function obtains total horizontal sediment flux q (units of g m^{-1} day^{-1}). An analysis of variance (ANOVA) was conducted to deduce significant differences of sediment flux and erosion bridge heights among the downwind plots in different sampling periods. A post hoc comparison of means following a significant ANOVA was done with a Tukey's studentized range test. To describe the general distribution of nutrients in soil samples, the mean, standard deviation, and coefficient of variation (CV) were also computed on both the deposition-enhanced plots (TD100) and control plots for both

sites over the experimental period. For each soil constituent, modified paired *t*-tests using PASSAGE software (http://www.passagesoftware.net/) were conducted to compare the mean values for the treatment plots (TD100) and control plots in both study sites. This modified *t*-test corrects the degrees of freedom considering the amount of autocorrelation in the data (Wang et al. 2007). All of these analyses were carried out using the program SAS 9.1 for Windows with $p<0.05$ for significance.

Geostatistical analysis was used to evaluate the spatial variation of N_{avail}, PO_4^{3-}, K^+, and Ca^{2+} in the TD100 and the control plots. Available N, PO_4^{3-}, and K^+ were selected because they are the limiting biological nutrients in desert ecosystems, especially N_{avail} and PO_4^{3-} (Crawford and Gosz 1982). Although Ca^{2+} content is high enough to not limit plant productivity in desert grasslands, chemicals related to Ca^{2+}, such as calcium carbonate, have a profound influence on the availability of other nutrients through a variety of biogeochemical processes (e.g., ammonia volatilization and neutralization of aid components) (Schlesinger et al. 1990).

The semivariogram is central to many geostatistical techniques; it shows the average variance found in analyses of samples taken at increasing distances from one another. Experimental semivariograms were fit using the jackknife method presented by Shafer and Varljen (1990) and discussed by Huisman et al. (2003) in a code written in the Interactive Data Language (IDL). Soil data sets were adjusted to approximate a normal distribution using a natural logarithmic transformation prior to analysis (Webster and Oliver 2000). Isotropic and corresponding anisotropic semivariograms at 0°, 45°, 90°, and 135° were compared, and no significant directional patterns were found. Therefore, isotropic semivariograms were used. We used the lag interval (distance increment) of 0.25 m and lag distance (maximum interval) of 4.0 m to calculate the experimental semivariograms for soil nutrients measured in July 2004, and a slightly larger lag interval (up to 0.35 m) and lag distance (up to 5.0 m) were used to better describe the potential change of soil spatial distributions in July 2006. All semivariograms were fit to a spherical model using a non-linear least squares approach employing the Levenberg-Marquardt algorithm, which combines the steepest descent and inverse-Hessian function fitting methods (Press et al. 1992). In the spherical model, if $h \leq A_0$, then $\gamma(h) = C_0 + C(\frac{3h}{2A_0} - \frac{h^3}{2A_0^3})$, where h is the lag interval, $\gamma(h)$ is the semivariance at lag interval h, A_0 is the range, C_0 is the nugget variance, and C is the structural variance. If $h > A_0$, then $\gamma(h) = C_0 + C$. The nugget (C_0) denotes the y-intercept of the semivariogram and incorporates random or non-spatial errors, as well as errors associated with spatial variability at scales finer than those measured (Zhou et al. 2008). A high nugget variance indicates that most variance occurs over short distances or is due to measurement/locational error (Schlesinger et al. 1996). The magnitude of spatial dependence was calculated using the index of $C/(C_0+C)$. As this index approaches 1.0, a greater proportion of the total sample variance is spatially structured (Jackson and Caldwell 1993). The distance of the spatial dependence is indicated by the model range, A_0. Samples separated by distances smaller than the range are correlated as a result of their proximity to one another, whereas samples separated by greater distances are effectively independent. The uncertainties (95% confidence limits) of variogram parameters were determined using the variance-covariance method of Pardo-Iguzquiza and Dowd (2001). In this research, variogram parameters are considered significantly different if they do not have overlapping 95% confidence intervals. After semivariance analysis, we produced kriged maps of N_{avail} using calculated semivariograms (GS^+ version 7.0, Gamma Design Software, Plainwell, Michigan) to examine how the predicted distribution of N_{avail} related to the distribution of fertile islands and plants in deposition-enhanced vs. control plots. Maps were produced using ordinary block kriging with a block size of 2 m×2 m. The data that were log-normally transformed were converted back to original units prior to kriging (Wang et al. 2007).

Results

Environmental conditions, sediment flux, and soil deposition

In comparison with the long-term (1915–2002) average of mean annual precipitation (247 mm), both year 2004 and 2006 were significantly wetter (389 mm and 416 mm, respectively), while year 2005 had a total rainfall (246 mm) nearly identical to the long-term average (Fig. 2a). However, during the

windy seasons (March-May), year 2006 was particularly dry with a total rainfall of less than 20 mm. The averaged 5 min maximum wind speed frequently exceeded 16 m s^{-1} during the windy season of 2006, with a peak speed of 21 m s^{-1} occurring on April 15th. These numbers are substantially higher than those of year 2004 and 2005 (Fig. 2b). Sediment flux monitoring suggested that dominant wind erosion occurred during the period of March to July in the experimental years (Fig. 2c). With the reduction of grass cover in the upwind area and resultant sediment flux of nearly 500 g m^{-1} day^{-1}, aeolian flux in the plots downwind of the vegetation-removal treatment (TD100) was substantially enhanced compared to that of the control plots. In particular, sediment flux monitored from March to July (collected in July) was significantly greater ($p<0.05$) in the TD100 plots than that of the control plots in both study sites. However, no significant differences were found for the sediment flux between the TD100 and control plots in March when there was little wind erosion at the JER. In addition, there were no significant sediment flux

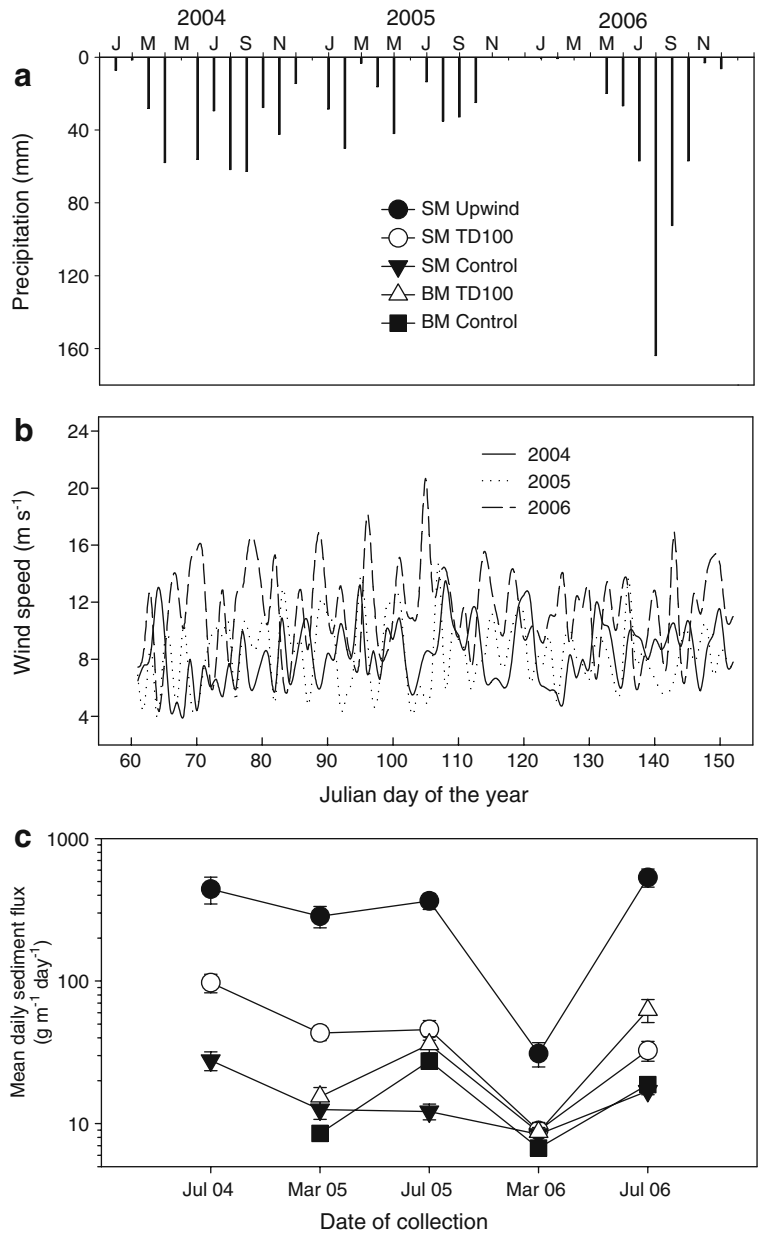

Fig. 2 Monthly precipitation (**a**), 5-min maximum wind speed (March 1-May 30, 10 m) (**b**), and mean daily horizontal sediment flux at the deposition enhanced plots (TD100) and control plots in both the *Sporobolus*-mesquite site (SM) and *Bouteloua*-mesquite site (BM) (**c**) during the experimental period (2004–2006). Sediment flux in the upwind grass cover reduction area was also included (SM upwind) as a comparison, data were adopted from Li et al. (2007). Error bars are one standard error. Note the legend for figure (**c**) was listed in figure (**a**) to facilitate figure arrangement

differences between the SM site and the BM site, except for July 2006 when mean sediment flux in the BM site (63 g m^{-1} day^{-1}) nearly doubled the magnitude of the SM site (34 g m^{-1} day^{-1}).

Erosion bridge results show that enhanced aeolian flux caused sediment deposition in the downwind treatment plots (Fig. 3). The average deposition rate, however, decreased rapidly as distance from the upwind/downwind boundary increased, corresponding with the significant decline of sediment flux from subplots D1 to D2. Significant deposition in the treatments (TD100) relative to the control plots occurred only in the D1 subplots of the SM site (paired *t*-test, $t=-1.95$, df=14, $p=0.03$), which is about 5 m from the upwind/downwind boundary. Average deposition measured in the D1 subplots was 0.61 cm

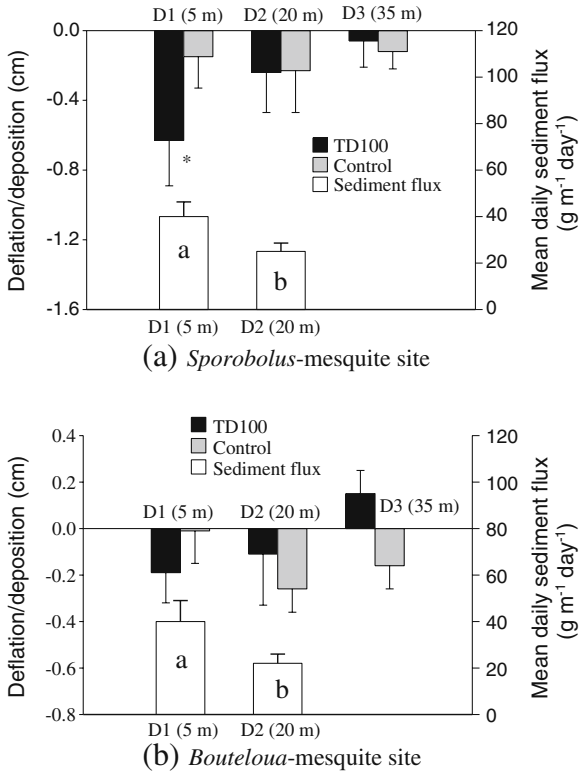

Fig. 3 Yearly mean deflation (cm yr^{-1}, negative) and deposition (positive) monitored by the erosion bridges in both study sites. Sediment flux in the D1 and D2 subplots are also shown (lower horizontal and right vertical axles). Numbers in the parentheses are distance from the subplot to the dividing line of the upwind-downwind. Error bars are one standard error. Significant difference in the sediment flux was indicated by different letters; significant difference in the hight of deposition/deflation between the TD100 and control plots was shown as "*" (paired *t*-test, $p<0.05$)

year^{-1} in the SM site, and substantially lower (0.21 cm year^{-1}) in the BM site.

Plot-scale heterogeneity of soil nutrients

At the beginning of the experiment, the mean values of N_{avail}, PO_4^{3-}, K^+, Mg^{2+}, Ca^{2+}, and Na^+ were significantly higher in the TD100 than in the control plot at the SM site; but only N_{avail} was more concentrated in the TD100 relative to the control plot at the BM site (Table 2, paired *t*-test, $p<0.05$). In the SM site after two windy seasons, the mean values for a large number of soil nutrients declined in the treatment plot (TD100) while they increased slightly in the control plots, causing the disappearance of significant difference in N_{avail}, Mg^{2+}, Ca^{2+}, and Na^+ between the TD100 and the control plots. In the BM site, the significantly higher concentration of N_{avail} in the TD100 compared to that of the control plot sustained after two windy seasons, while no other significant changes were observed.

Before the initiation of enhanced deposition, the overall variation of soil nutrients in the SM site was generally greater than that of the BM site (Table 3). In both study sites, CVs were always highest for soluble ions such as SO_4^{2-} and Cl^-, and lowest CVs were mostly found for ions such as PO_4^{3-}, Mg^{2+}, and Ca^{2+}. After 2 years of enhanced deposition, the ratios of CV between the TD100 and control plots for N_{avail}, PO_4^{3-}, Cl^-, and Na^+ decreased markedly in the SM site, largely due to the decline of overall variability in the treatment plot (TD100) and a slight increase in the CVs in the control plot. A similar change occurred in the BM site during this period, except that a larger CV was found for Na^+. Overall in TD100, CVs for cations were relatively low and changed slightly; CVs for N_{avail}, SO_4^{2-}, and Cl^- were high and decreased substantially with the continuation of deposition.

Spatial heterogeneity of soil nutrients

The Sporobolus-mesquite site (SM)

At the beginning of the experiment (July 2004), most of the soil nutrients studied were highly to moderately spatially dependent with $C/(C_0+C)$ >50%, except for Ca^{2+} in the control plot ($C/(C_0+C)$=39%). In the TD100 plot, all the soil nutrients examined were autocorrelated over mean distances (A_0) of 1.27–

Table 2 The mean concentration of soil nutrients measured in the deposition enhanced plots (TD100) and control plots (C) during the experimental period

Nutrients (mg kg^{-1})	*Sporobolus*-mesquite site				*Bouteloua*-mesquite site			
	July 2004		July 2006		July 2004		July 2006	
	TD100	C	TD100	C	TD100	C	TD100	C
N_{avail}	24.26	17.18	17.24	19.88	39.36	11.63*	29.85	17.61*
PO_4^{3-}	6.01	7.18*	5.66	7.20*	3.95	4.59	4.35	4.30
K^+	155.70	96.53*	155.73	107.59*	136.95	146.84	143.37	137.66
Mg^{2+}	98.38	52.32*	90.68	54.21	61.45	65.26	56.75	66.91
Ca^{2+}	545.92	431.10*	504.90	482.25	998.57	973.23	1006.48	1034.48
SO_4^{2-}	3.29	3.75	1.74	3.57	3.30	4.06	2.22	2.32
Cl^-	1.15	0.84	0.46	1.19	1.02	1.40	0.44	0.77
Na^+	6.54	3.11*	3.40	4.20	5.50	3.18	2.98	2.82

*Indicates a significant difference in the mean concentrations between deposition enhanced plots (TD100) and the control plots in different sampling years (paired *t*-test, $p < 0.05$)

1.50 m. In contrast, soil nutrients in the control plot were autocorrelated over slightly smaller distances of 0.89–1.36 m, but they were not significantly different from those of the TD100 plot. The autocorrelation distances of soil nutrients in both plots fell within the range of the average size of shrub canopies in the study sites, which are 1.62±0.28 m and 1.89±1.00 m in the T100 and control plots, respectively (Table 1). Overall, both A_0 and $C/(C_0+C)$ were not significantly different between the TD100 and the control plots before the initiation of enhanced sediment deposition (Table 4a).

After 2 years of enhanced sediment deposition (July 2006), soil PO_4^{3-} in the TD100 plot and Ca^{2+} in the control plot changed from patterned to random distribution with most of the variance occurring over distances <0.3 m. For soil nutrients with patterned distribution, the mean scale of autocorrelation (A_0) for soil Navail increased significantly from 1.50 m (July 2004) to 1.81 m (July 2006) in the treatment plot (TD100) comparing with A0 in the control plot during the same period. In the meantime, the magnitude of spatial dependence ($C/(C_0+C)$) in the TD100 plot did not show significant changes relative to that of the control plot during the experimental period.

The kriging maps show that soil N_{avail} exhibited strong fertile islands in both the TD100 and control plots at the beginning of the experiment (Fig. 4a). In addition, N_{avail} islands in the TD100 plot are largely located in the left half of the subplot, which is comparable to the distribution of mesquites (Fig. 8a). After 2 years of enhanced deposition, the size of N_{avail}

Table 3 Changes of coefficient of variation (100% (SD/Mean)) for the overall concentration of soil nutrients at both sites during the experimental period ($n=50$)

Nutrients (mg kg^{-1})	*Sporobolus*-mesquite site (SM)						*Bouteloua*-mesquite site (BM)					
	July 2004			July 2006			July 2004			July 2006		
	TD100	C	Ratio	TD100	C	Ratio	TD100	C	Ratio	TD100	C	Ratio
N_{avail}	107	108	0.99	78	99	0.79	71	77	0.92	47	123	0.38
PO_4^{3-}	37	44	0.84	27	45	0.60	27	27	1.00	16	33	0.48
K^+	39	33	1.18	39	51	0.76	28	32	0.88	23	33	0.70
Mg^{2+}	22	26	0.85	24	21	1.14	22	28	0.79	23	19	1.21
Ca^{2+}	16	15	1.07	17	24	0.71	12	20	0.60	11	24	0.46
SO_4^{2-}	136	158	0.86	163	211	0.77	66	186	0.35	50	186	0.27
Cl^-	158	105	1.50	206	324	0.64	88	293	0.30	72	339	0.21
Na^+	156	24	6.50	22	94	0.23	11	14	0.79	24	16	1.50

Table 4 Summary of the semivariogram model parameters in both study sites before (July 2004) and after enhanced deposition (July 2006)

Nutrients	A_0 (m)		$C/(C_0+C)$	
	TD100	Control	TD100	Control
(a) *Sporobolus*-mesquite site (SM)				
July 2004				
N_{avail}	1.50 (0.32)	1.36 (0.48)	1.00 (0.10)	1.00 (0.34)
PO_4^{3-}	1.40 (0.34)	1.00 (0.48)	0.73 (0.10)	0.58 (0.25)
K^+	1.48 (1.09)	0.89 (0.54)	0.52 (0.26)	1.00 (0.25)
Ca^{2+}	1.27 (0.53)	0.99 (0.53)	0.58 (0.11)	0.39 (0.61)
July 2006				
N_{avail}	1.81 (0.40)*	0.89 (0.27)	0.88 (0.13)	1.00 (0.47)
PO_4^{3-}	<0.3	1.43 (0.34)	-	1.00 (0.24)
K^+	1.25 (0.37)	1.74 (0.53)	1.00 (0.28)	0.78 (0.21)
Ca^{2+}	1.10 (0.42)	<0.3	1.00 (0.75)	-
(b) *Bouteloua*-mesquite site (BM)				
July 2004				
N_{avail}	3.01 (0.93)*	0.62 (0.52)	0.48 (0.14)	1.00 (0.61)
PO_4^{3-}	2.51 (0.86)	3.82 (2.16)	0.51 (0.20)	0.52 (0.21)
K^+	1.63 (0.25)	1.84 (0.72)	0.79 (0.14)	0.59 (0.27)
Ca^{2+}	4.51 (2.83)*	1.16 (0.28)	0.33 (0.22)	0.95 (0.12)
July 2006				
N_{avail}	3.81 (1.63)*	1.08 (0.51)	0.55 (0.20)	1.00 (0.67)
PO_4^{3-}	1.78 (0.53)	2.12 (1.82)	0.65 (0.18)	0.35 (0.19)
K^+	<0.3	1.25 (0.30)	-	1.00 (0.19)
Ca^{2+}	1.25 (0.74)*	>5.00	0.49 (0.28)	0.18(0.14)

Results for $C/(C_0+C)$ and A_0 are means and 1 standard deviation (in the parentheses). "-"indicates random distribution and no data available. Asterisks indicate significant differences between deposition enhanced vs. control plots at a 95% confidence level

fertile islands in the TD100 plot increased slightly, whereas peak values of the islands decreased substantially from 127 mg kg^{-1} to 67 mg kg^{-1}. In the control plot, both the scale and the peak values of N_{avail} islands changed to a small degree except for their locations. Change maps of N_{avail} further illustrate that N_{avail} declined in the dominant portion of the deposition enhanced plot, while N_{avail} increased noticeably in most part of the control plot (Fig. 5a).

The Bouteloua-mesquite site (BM)

Similar to the SM site, soil nutrients showed moderate spatial dependency in July 2004. The scale of autocorrelation ranged over mean distances of 0.62 m (N_{avail}, control plot) to >5 m (Ca^{2+}, TD100 plot). Overall, soil nutrients in the BM site frequently showed greater autocorrelation distances than those in the SM site, which is probably not related to the spatial distribution of shrubs, but rather to the larger basal area of Bouteloua individuals compared to Sporobolus individuals in the plots (Table 4b).

By July 2006, the scale of the autocorrelation (A_0) of N_{avail} in both the TD100 and the control plots increased by a small degree; however, significant difference in A_0 between these two plots was maintained. The magnitude of spatial dependence changed little except for Ca^{2+} in the TD100, which changed from a moderate spatial dependency of 33% in July 2004 to a non-patterned distribution at the scale investigated after two windy seasons.

Kriged maps illustrated that N_{avail} formed weak islands in both the TD100 and the control plots in July 2004 (Fig. 4b), corresponding to the infrequent distribution of shrubs in the study site (Fig. 8b). N_{avail} spatial patterns were fairly stable after two windy seasons in the TD100 plot. In the control plot, the appearance of a N_{avail} island in the middle part of the kriged map in July 2006 may be corresponding with the presence of a mesquite (Fig. 8b). The magnitude

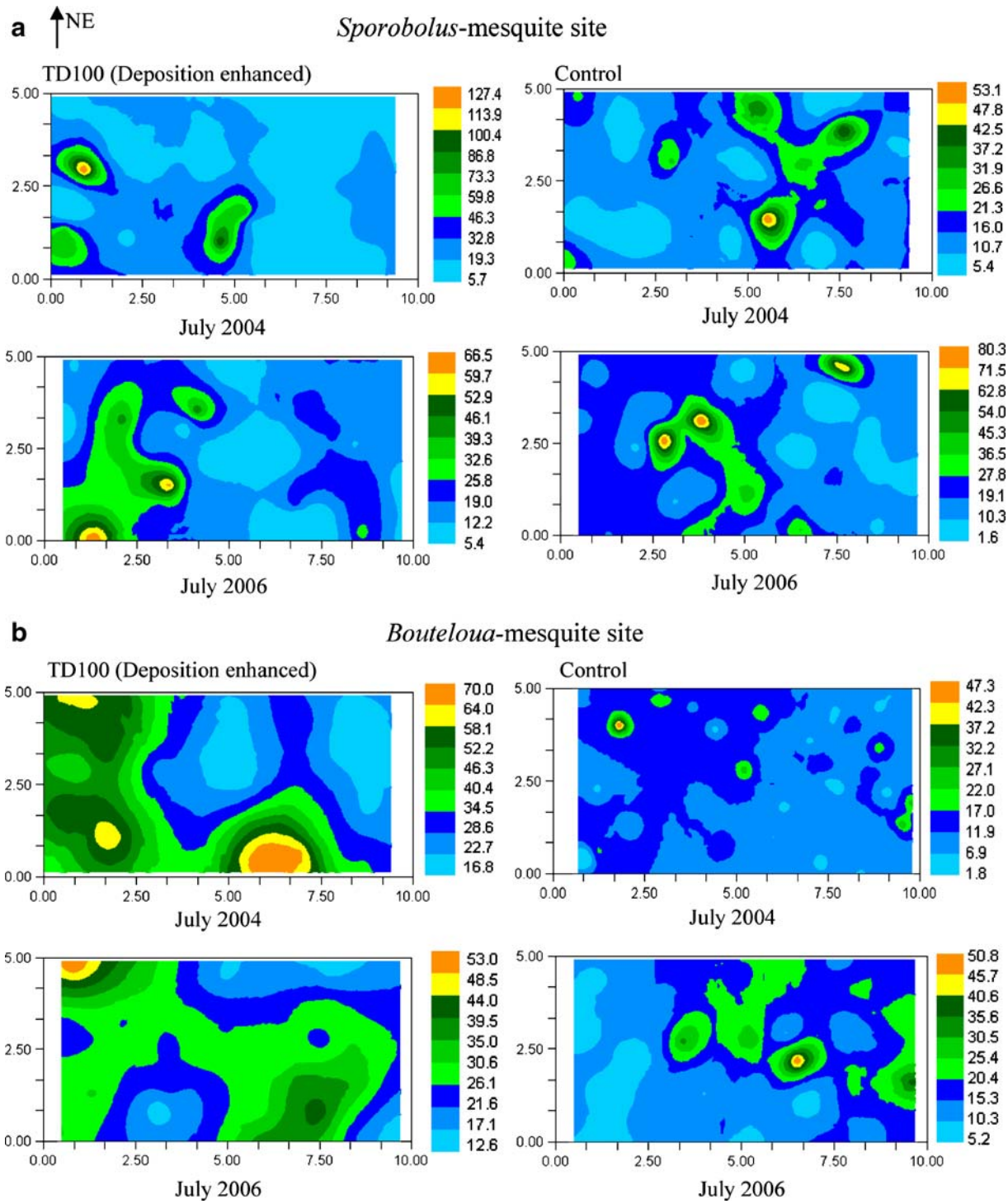

Fig. 4 Distribution of N_{avail} (mg kg^{-1}) predicated by kriging interpolation in the deposition enhanced (TD100) and the control plots (5 m×10 m) at both sites during the experimental period. Note the change of the scales in the treatment plots

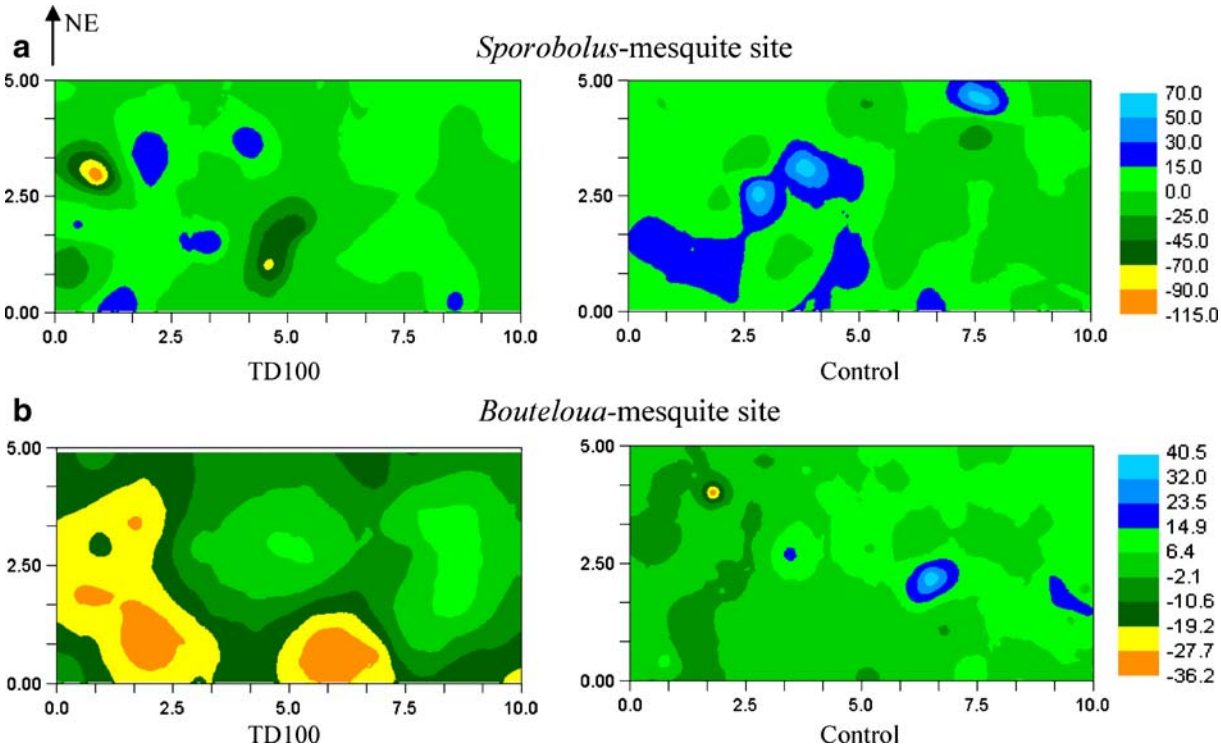

Fig. 5 Change of N_{avail} (mg kg^{-1}) in the treatment (TD100) and control plots (5 m × 10 m) during the experimental period. Maps were obtained by subtracting values in 2004 from 2006 (Fig. 4), and negative values indicating depletion. Same scales were used for the treatment and control plots in each site to facilitate comparison

of N_{avail} concentration change in the BM site was -36.2 to 45.6 mg kg^{-1}, which is substantially smaller than that of the SM site (−115−70 mg kg^{-1}) (Fig. 5b). Similar to the SM site, N_{avail} in the BM site decline in most of the TD100 plot but increased slightly in the majority of the control plot.

Discussion

Most previous plot-scale research on aeolian processes and their interactions with soil and vegetation processes have focused on erosion and soil nutrient loss in arid and semiarid regions (e.g., Leys and McTainsh 1994; Larney et al. 1998; Li et al. 2007, 2008; Gillette and Pitchford 2004). Studies that have quantitatively investigated sand and dust deposition and their biogeochemical consequences in ecosystems on a plot-scale are rare. In the two desert grassland ecosystems downwind of erosion-enhanced plots, we monitored sediment flux and deposition with multiple BSNEs, erosion bridges, and intensive surface soil sampling. Li et al. (2007) calculated sand drift potential in the upwind plots and found that sand particles, which compose the greatest portion of the mass flux, indeed moved along the long axis of the vegetation removal treatments. Results from this study further suggest that net sediment deposition was pronounced in the two-year experimental period, and the deposition rate may be related to the local plant community composition. In particular, despite similar horizontal sediment flux (500 g m^{-1} day^{-1}) in both upwind erodible plots (Li et al. 2007, 2008), average net depositions of 0.61 and 0.21 cm $year^{-1}$ were observed in the plots with dominant grasses of *Sporobolus* spp. (SM site) and *Bouteloua eriopoda* (BM site), respectively.

Using the method of McGlynn and Okin (2006) and Total Station data to calculate the average size of bare patches in plots, the average gap size in the SM site is ~123 cm, and the average gap size in the BM site is ~ 88 cm. In a new model of wind erosion, Okin (2008) hypothesized that the amount of horizontal flux that could be sustained on a vegetated surface

was related to the size of unvegetated gaps between plants. All other things being equal, according to this model, the SM site with its larger gaps between plants could sustain higher rates of horizontal flux than the BM site. Of course, the horizontal flux of sand entering the upwind edge of both sites, having been generated on a bare surface with very large intercanopy gaps, is higher than can be sustained on the vegetated portions of either site. Within the vegetated plots, the high flux entering the plot must re-equilibrate with the vegetated surface that can only support lower flux. This results in the deposition of windblown material at the upwind edge of the plots, which decreases as the distance from the edge increases.

Thus, because the gap size is smaller on the BM site, causing the potential horizontal flux also to be smaller, the deposition rate of windblown material should be higher in the BM site. However, we believe that much of this deposition would occur rapidly as the material entered the area with vegetation. And much of the erosion thus occurred upwind of the erosion bridges placed 5 m downwind of the boundary (Fig. 6). Given that the present experiment provides only two data points, we suggest that more research would be required to clarify the relationship between flux, deposition, and gap size in depositional areas.

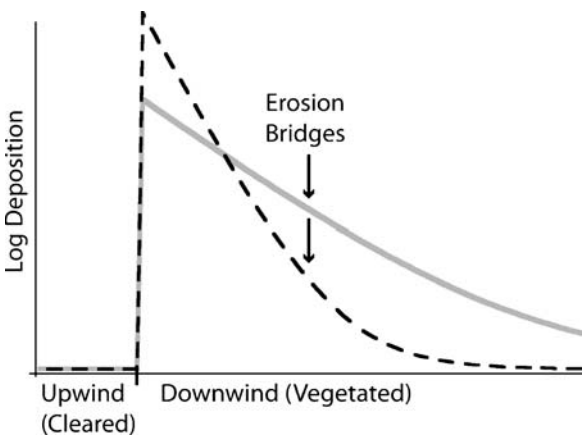

Fig. 6 Hypothesized, schematic profile of deposition from upwind, cleared area (*left*) to downwind vegetated area (*right*). It is believed that flux entering the BM vegetated area with smaller gaps between plants results in more rapid deposition (*dashed line*) than flux entering the SM vegetated area with larger gaps between plants (*solid line*). In this scenario, measurement of deposition at some downwind points (i.e., where we placed erosion bridges) would result in apparently higher deposition on plots with large gaps compared to deposition on plots with small gaps

Okin et al. (2001) presented a conceptual model to explain ecosystem changes observed in the downwind area of the scraped site at the JER, focusing on differential physiological responses of shrubs and grasses to the physical effects (e.g., burial and abrasion) of windblown sand and dust particles (Fig. 7). The conceptual model further suggests that surface soil in downwind depositional areas may become depleted in nutrients. However, these authors did not present quantitative estimates of soil nutrient content and spatial heterogeneity changes caused by enhanced deposition. Results of this study agreed with the conceptual model and showed that surface soil generally became nutrient-poor after 2 years of enhanced deposition; however, the degree of decline was not equivalent across various nutrient constituents (Table 2). Labile ions such as N_{avail}, SO_4^{2-}, Cl^-, and Na^+ declined most notably, while soil PO_4^{3-}, K^+, Mg^{2+}, and Ca^{2+} changed little over this 2-year period. The different responses of soil nutrients to aeolian processes have also been observed in the erosion-enhanced upwind area in a previous study by Li et al. (2008).

Study of wind physics suggests that materials deposited in the downwind and proximate area are comprised mostly of saltating sands with particle diameter greater than 50 μm (Okin et al. 2006). Li et al. (2006) analyzed soil particle distributions and their associated nutrient content in the airborne sediment at 0.3 m height at the JER. The authors found that soil particles of 125–500 μm account for 85% of the mass, but account for less than 60% of the total N content. In contrast, soil particles with diameter <50 μm account for <1% of mass but contribute >10% of total N. Larney et al. (1998) found that N_{avail} concentrations in windborne sediments collected at the height of 0.25 m in semiarid Canadian grasslands were only 50% of the surface soil N_{avail} concentrations, while Mg^{2+} and Ca^{2+} concentrations in the sediment were nearly identical to those of the surface soil. Therefore, we suggest that particles deposited in the downwind area may be particularly poor in labile ions such as SO_4^{2-}, Cl^-, Na^+, and N_{avail}, but the concentrations of immobile nutrients like PO_4^{3-}, Mg^{2+}, and Ca^{2+} are unaffected. The deposition of this "nutrient-imbalanced" soil may affect the ecological and physiological performance of plant species. The low

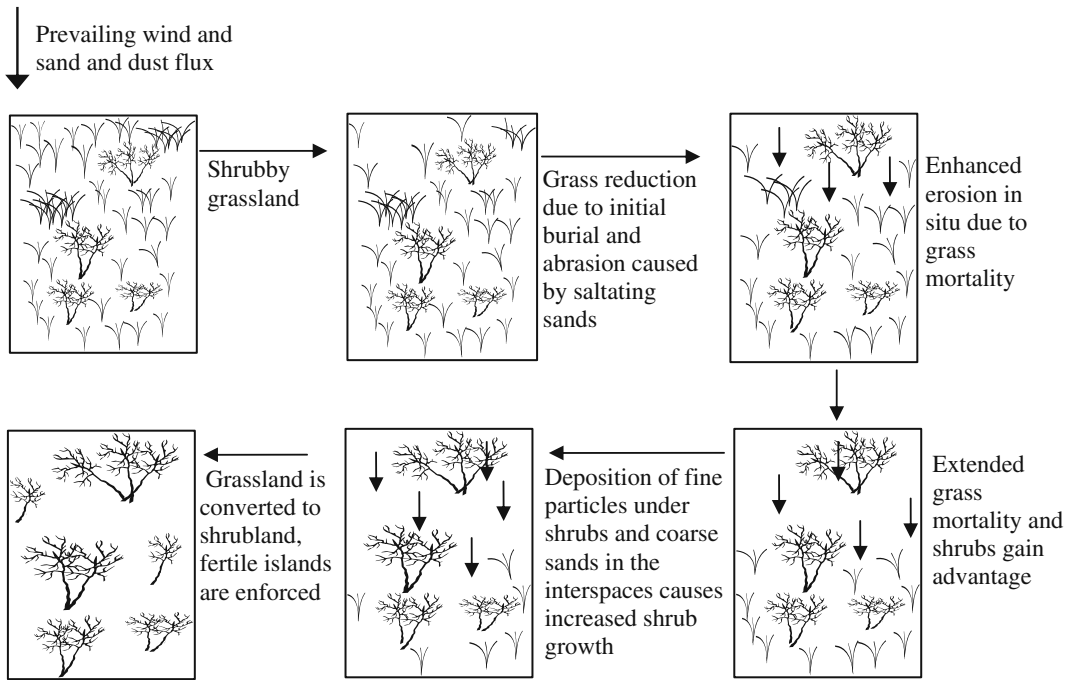

Fig. 7 A conceptual model showing the role of wind in the conversion of shrubby grassland to shrubland in a deposition enhanced environment. Revised from Okin et al. (2001) and Hartman et al. (2006)

NO_3^- -N content in the deposited sand may limit the germination of grass seeds, since NO_3^- -N is known to stimulate seed germination (Karssen and Hilhorst 1992). Some shrubs, however, may not suffer from the low N sand, since they are relatively efficient users of N (e.g. *Larrea tridentata*), or have symbiotic associations with nitrogen-fixing organisms (e.g. *Prosopis glandulosa*) (Lajtha and Schlesinger 1986).

The competition advantage of shrubs over grasses in this deposition dominant environment may be further illustrated in Fig. 8. In combination with their natural growth, Total Station data showed that the mean canopy size of mesquites in the TD100 plot of the SM site increased from 1.97 m in July 2004 to 2.30 m in July 2006, while the mean size of the only mesquite in the D1 subplot of the TD100 plot at the BM site grew from 0.25 m to 0.61 m in the same period. However, mesquite canopy size in the control plots was largely unchanged during the same period. In addition, the mortality of grasses and *Gutierrezia* in the deposition-enhanced plots at both sites was visible, particularly in the BM site, where initial grass cover was substantially higher than in the SM site.

Despite the substantial diminishment in the mean content of several soil nutrients, the spatial distribution of the soil resources may be more important than mean values in determining the vegetation pattern and its dynamics in arid and semiarid environments (Schlesinger et al. 1990). Very few studies have continuously monitored soil nutrient variation in an erosion/deposition environment. Okin et al. (2001) suggest that soil heterogeneity may be increased in the deposition enhanced area due to the trapping of nutrient-enriched windborne particles by shrubs and the deposition of coarse, nutrient poor material in the interspaces (Fig. 7). Our results of CVs, however, show that the overall variation of several soil nutrients decreased (e.g., N_{avail}, PO_4^{3-}, SO_4^{2-}, and Cl^-) or changed little (e.g., K^+, Mg^{2+}, and Ca^{2+}) with enhanced wind erosion (Table 3). These results may suggest that during the first 2 years of this study, sand supply for wind erosion in the upwind area is "unlimited," and deposition of large-sized saltation

Fig. 8 Distribution of plants in the 5 m×10 m soil sampling subplots in the deposition enhanced (TD100) and control plots in both study sites during the experimental period. The size of the symbols represents the approximate size of the plants

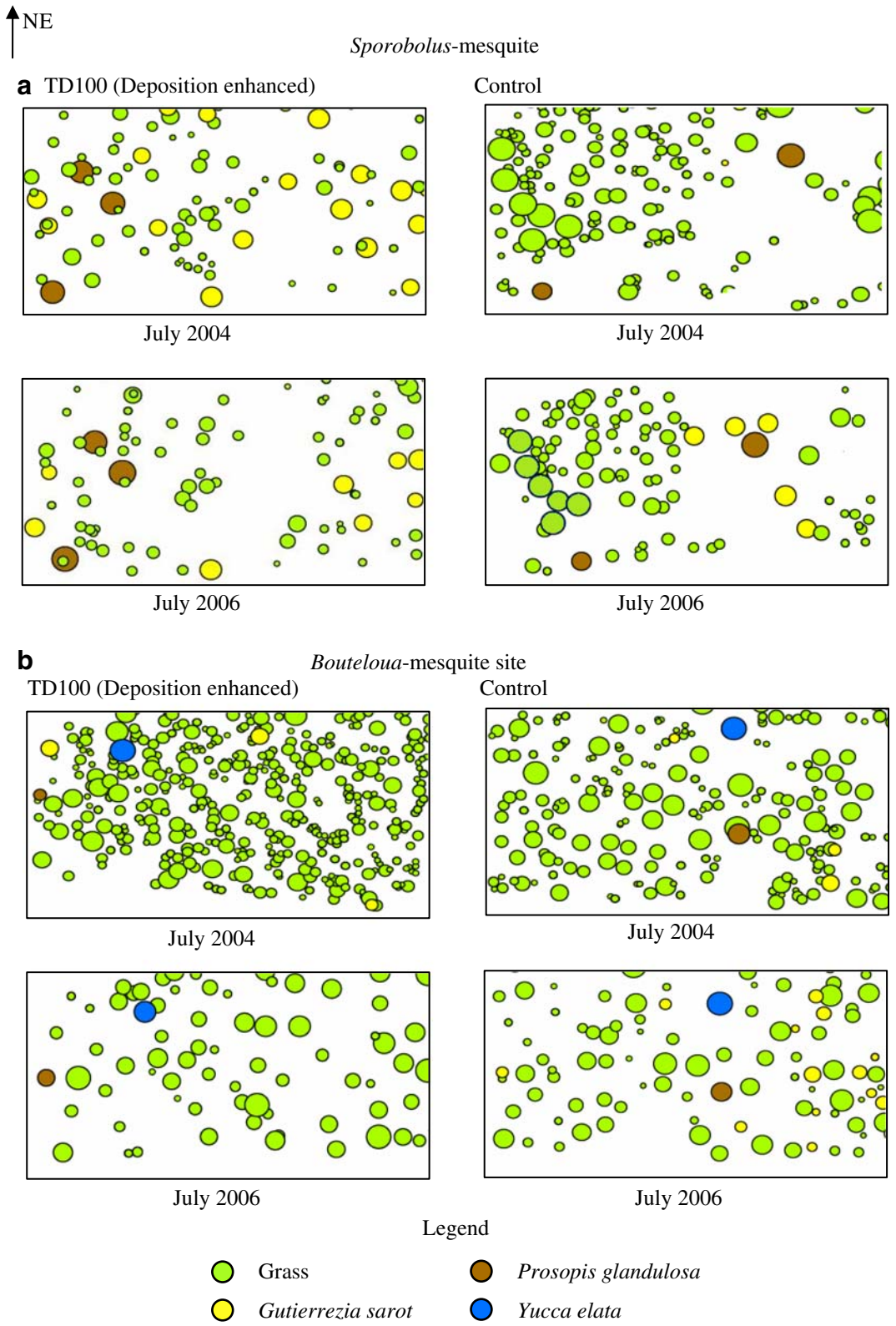
NE
Sporobolus-mesquite
a TD100 (Deposition enhanced)
Control
July 2004
July 2004
July 2006
July 2006
b
Bouteloua-mesquite site
TD100 (Deposition enhanced)
Control
July 2004
July 2004
July 2006
July 2006
Legend
Grass
Prosopis glandulosa
Gutierrezia sarot
Yucca elata

particles is predominant compared to the trapping of fine, nutrient-rich particles by shrubs.

Geostatistics allowed us to quantitatively infer the degree and scale of spatial dependence in the distribution of soil nutrients, and changes in their spatial heterogeneity associated with enhanced sediment deposition. In July 2004, most of the soil nutrients are spatially dependent at a scale <2 m in the SM site (dominated by *Prosopis glandulosa* and *Sporobolus spp*) and up to 4.51 m (Ca^{2+} in TD100) in the BM site (dominated by *Bouteloua eriopoda)* (Table 4a,b). The scale of spatial dependence corresponds well with the range reported in other semiarid grasslands. Schlesinger et al. (1996) report that N_{avail} was spatially dependent at mean distances of 6.0 m and 2.0 m in grassland and shrubland sites at the JER, respectively. Zhou et al. (2008) found that soil organic C and N displayed autocorrelation over a range ~2 m in a semiarid grassland of Inner Mongolia, northern China. Results of this study are also consistent with the finding that grassland under a uniform cover usually processes a longer spatial autocorrelation in soils than in areas of woody vegetation (Schlesinger et al. 1996). Shorter ranges of autocorrelation for soil nutrients in the SM site are likely due to the fact that biotic processes are acting at the scale of individual shrubs (Schlesinger et al. 1996). Døckersmith et al. (1999) further pointed out that plants may influence the spatial distribution of soil nutrients through litter deposition and decomposition, stemflow, and throughfall.

In the two desert grasslands we studied, enhanced sediment deposition did not appear to affect the degree of spatial dependence significantly in soil nutrients over a 2-year period (Table 4b). However, enhanced deposition increased the scale of variability of N_{avail} at the SM site (Table 4b). For example, the range of N_{avail} increased from 1.50 m in July 2004 to 1.81 m in July 2006 in the TD100 plot, while during the same period the autocorrelation scale of N_{avail} decreased from 1.36 m to 0.89 m in the control plot. The kriged maps visibly show the transformation of N_{avail} in the deposition enhanced plots over the experimental period. In the SM site, strong soil N_{avail} islands were largely maintained; but in the BM site with substantially higher cover of *Bouteloua eriopod*, the originally fragmented and relatively strong N_{avail} islands have been replaced by more diffuse and weak resource islands (Fig. 4). These results suggest that the spatial heterogeneity of soil nutrients in a *Bouteloua* grass-dominated community may be more susceptible to change under enhanced sand and dust deposition than a *Sporobolus* grass-dominated community in the desert grassland of Jornada.

In summary, our results showed that enhanced deposition led to considerable reduction in both mean soil nutrient concentrations and CVs in the sandy soils of the JER over a 2-year period (2004–2006). Given the observed increase in the scale of spatial dependence for N_{avail}, but not for K^+, PO_4^{3-}, and Ca^{2+} following enhanced sediment deposition, we suggest that this plant limiting nutrient (N_{avail}) may be particularly responsive to increased soil erosion due to livestock grazing and other anthropogenic activities that remove vegetation. Our study further suggests that soil particles deposited in the downwind area may be "nutrient-imbalanced." Specifically, the lower-than-normal N_{avail} concentrations in the wind-deposited soils may inhibit the growth of grasses and the germination of seeds. Based on the results for wind-erodible ecosystems found in southern New Mexico, *Bouteloua*-dominated communities may be particularly susceptible to change under enhanced soil erosion conditions.

Acknowledgements This research was supported by the National Science Foundation (DEB No. 0316320) and Long-Term Ecological Research Grant (DEB No. 0080412). We are grateful to Jacquie Hui, Mike Abrams, Emilee Carpenter, Melissa Castiano, Steve Pacenka, and Tom Zhao for their assistance in field work, laboratory analysis, and data processing. We also appreciate the JER headquarters of the US Department of Agriculture-Agricultural Research Service staff Kris Havstad, John Anderson, Eddie Garcia, Rob Dunlap, and David Thatcher, who provided invaluable assistance with field work during this study. The insightful comments from two anonymous reviewers have significantly improved the quality of this work.

References

Ayoub A (1998) Extent, severity and causative factors of land degradation in the Sudan. J Arid Environ 38(3):397–409 doi:10.1006/jare.1997.0346

Barth HJ (1999) Desertification in the eastern province of Saudi Arabia. J Arid Environ 43(4):399–410

Bulloch HE Jr, Neher RE (1977) Soil survey of Dona County area, New Mexico. Soil Conserv. Serv., U. S. Dep. of Agric., Washington, DC

Chadwick OA, Derry LA, Vitousek PK, Huebert BJ, Hedin JO (1999) Changing sources of nutrients during four million years of ecosystem development. Nature 397:491–497 doi:10.1038/17276

Coppinger KD, Reiners WA, Burke IC, Olson PK (1991) Net erosion on a sagebrush steppe landscape as determined by cesium-137 distribution. Soil Sci Soc Am J 55:254–258

Crawford CS, Gosz JR (1982) Desert ecosystems: their resources in space and time. Environ Conserv 9:181–195

Døckersmith IC, Giardina CP, Sanford RL Jr (1999) Persistence of tree related patterns in soil nutrients following slash-and-burn disturbances in the tropics. Plant Soil 209:137–156 doi:10.1023/A:1004503023973

Fryrear DW (1986) A field dust sampler. J Soil Water Conserv 41:117–120

Gillette DA, Chen WA (2001) Particle production and Aeolian transport from a supply-limited source area in the Chihuahuan desert, New Mexico, United States. J Geophys Res 106:5267–5278 doi:10.1029/2000JD900674

Gillette DA, Pitchford AM (2004) Sand flux in the northern Chichuhuan desert, New Mexico, USA, and the influence of mesquite-dominated landscapes. J Geophys Res 109: F04003 doi:10.1029/2003JF000031

Gillette DA, Monger HC (2006) Eolian processes on the Jornada Basin. In: Havstad KM, Huenneke LF, Schlesinger WH (eds) Structure and Function of a Chihuahuan Desert Ecosystem: the Jornada Basin Long-term Ecological Research Site. Oxford University Press, New York, USA, pp 189–210

Gillman GP, Bruce RC, Davey BG, Kimble JM, Searle PL, Skjemstad JO (1983) A comparison of methods used for determination of cation exchange capacity. Commun Soil Sci Plant Anal 14:1005–1014 doi:10.1080/00103628309367428

Griffin DW, Garrison VH, Herman JR, Shinn EA (2001) African desert dust in the Caribbean atmosphere: microbiology and public health. Aerobiologia 17:203–213 doi:10.1023/A:1011868218901

Hartman L, Epstein H, Okin G, Li J (2006) Wind erosion and vegetation interactions in a desert ecosystem. American Geophysical Union Fall Meeting, San Francisco, CA

Helm P, Breed CS (1999) Monitoring surface changes in desert areas. In: Breed CS, Reheis MC (eds) Desert Winds: Monitoring Wind-Related Surface Processes in Arizona, Mexico and California. US Geological Survey Professional Paper 1598. G.P.O., Washington, USA, pp 30–51

Hendershot WH, Duquette M (1986) A simple barium chloride method for determining cation exchange and exchangeable cations. Soil Sci Soc Am J 50:605–608

Horn OP, Alley MM, Bertsh PM (1982) Cation exchange capacity measurements. Commun Soil Sci Plant Anal 13:851–862 doi:10.1080/00103628209367315

Huisman JA, Snepvangers JJJC, Bouten W, Heuvelink GBM (2003) Monitoring temporal development of spatial soil water content variation. comparison ground penetrating radar time domain reflectometry. Vadose Zone 2:519–529

Jackson RB, Caldwell MM (1993) Geostatistical patterns of soil heterogeneity around individual perennial plants. J Ecol 81:683–692

Karssen CM, Hilhorst HWM (1992) Effect of chemical environment on seed germination. In: Fenner M (ed) Seeds-ecology of regeneration in plant communities. CAB International, Wallingford, UK, pp 327–348 pp 373

Lajtha K, Schlesinger WH (1986) Plant response to variations in nitrogen availabity in a desert shrubland community. Biogeochemistry 2:29–37

Larney FJ, Bullock MS, Janzen HH, Ellert BH, Olson ES (1998) Wind erosion effects on nutrient redistribution and soil productivity. J Soil Water Conserv 53(2):133–140

Leys J, McTainsh G (1994) Soil loss and nutrient decline by wind erosion-cause for concern. Aust J Soil Water Conserv 7(3):30–40

Leys JF, McTainsh GH (1996) Sediment fluxes and particle grain-size characteristics of wind-eroded sediments in southeastern Australia. Earth Surf Process Landf 21:661–671 doi:10.1002/(SICI)1096-9837(199607)21:7<661::AID-ESP663>3.0.CO;2-4

Li J, Okin GS, Alvarez L, Epstein H (2006) Impacts of wind erosion on the characteristics of sand and dust flux in southern New Mexico. American Geophysical Union Fall Meeting, San Francisco, CA

Li J, Okin GS, Alvarez L, Epstein H (2007) Quantitative effects of vegetation cover on wind erosion and soil nutrient loss in a desert grassland of southern New Mexico, USA. Biogeochemistry 85:317–332 doi:10.1007/s10533-007-9142-y

Li J, Okin GS, Alvarez L, Epstein H (2008) Effects of wind erosion on the soil nutrient heterogeneity in two desert grassland communities. Biogeochemistry 88:73–88 doi:10.1007/s10533-008-9195-6

McGlynn IO, Okin GS (2006) Characterization of shrub distribution using high spatial resolution remote sensing: ecosystem implication for a former Chihuahuan desert grassland. Remote Sens Environ 101:554–566 doi:10.1016/j.rse.2006.01.016

Neff J, Ballantine A, Farmer G, Mahowald N, Conroy J, Landry C, Overpeck J, Painter T, Lawrence C, Reynolds R (2008) Increasing eolian dust deposition in the western United States linked to human activity. Nature-Geosciences 1:189–195 doi:10.1038/ngeo133

Okin GS (2008) A new model of wind erosion in the presence of vegetation. J Geophys Res-Earth Surf 113:F02S10 doi:10.1029/2007JF000758

Okin GS, Gillette DA (2001) Distribution of vegetation in wind-dominated landscapes: implications for wind erosion modeling and landscape processes. J Geophys Res 106:9673–9683 doi:10.1029/2001JD900052

Okin GS, Murray B, Schlesinger WH (2001) Degradation of sandy arid shrubland environments: observation, process modeling and management implications. J Arid Environ 47:123–144 doi:10.1006/jare.2000.0711

Okin GS, Mahowald NM, Chadwick OA, Artaxo PE (2004) The impact of desert dust on the biogeochemistry of phosphorus in terrestrial ecosystems. Global Biogeochem Cycles 18(2). doi:10.1029/2003GB002145

Okin GS, Gillette DA, Herrick JE (2006) Multi-scale controls on and consequences of Aeolian processes in landscape change in arid and semi-arid environments. J Arid Environ 65:253–275 doi:10.1016/j.jaridenv.2005.06.029

Pardo-Iguzquiza E, Dowd P (2001) Variance-covariance matrix of the experimental variogram: assessing variogram uncertainty. Math Geol 33(4):397–419 doi:10.1023/A:1011097228254

Peters DPC, Bestelmeyer BT, Herrick JE, Monger HC, Fredrickson E, Havstad KM (2006) Disentangling complex landscapes: new insights to forecasting arid and semiarid system dynamics. Bioscience 56:491–501 doi:10.1641/0006-3568(2006)56[491:DCLNII]2.0.CO;2

Piketh SJ, Tyson PD, Steffen W (2000) Aeolian transport from southern Africa and iron fertilization of marine biota in the South Indian Ocean. S Afr J Geol 96:244–246

Press WH, Teukolsky SA, Vetterling WT, Flannery BP (1992) Numerical recipes in C: the art of scientific computing, 2ndnd edn. Cambridge University Press, Cambridge, p 944

Reheis MC (2006) A 16-year record of eolian dust in Southern Nevada and California, USA: controls on dust generation and accumulation. J Arid Environ 67:487–520 doi:10.1016/j.jaridenv.2006.03.006

Reynolds R, Belnap J, Reheis M, Lamothe P, Luiszer F (2001) Aeolian dust in Colorado Plateau soils: nutrient inputs and recent change in source. Proc Natl Acad Sci USA 98 (13):7123–7127 doi:10.1073/pnas.121094298

Schlesinger WH, Reynolds J, Cunningham G, Huenneke L, Jarrell W, Virginia R, Whitford W (1990) Biological feedbacks in global desertification. Science 247:1043–1048 doi:10.1126/science.247.4946.1043

Schlesinger WH, Raikes AF, Hartley AE, Cross AF (1996) On the spatial pattern of soil nutrients in desert ecosystems. Ecology 77:364–374 doi:10.2307/2265615

Shafer JM, Varljen MD (1990) Approximation of confidence-limits on sample semivariograms from single realizations of spatially correlated random-fields. Water Resour Res 26(8):1787–1802

Shao Y, Raupach MR, Findlater PA (1993) The effects of salation bombardment on the entrainment of dust by wind. J Geophys Res 98:12719–12726 doi:10.1029/93JD00396

Wang L, Mou PP, Huang J, Wang J (2007) Spatial heterogeneity of soil nitrogen in a subtropical forest in China. Plant Soil 296:137–150 doi:10.1007/s11104-007-9271-z

Webster R, Oliver MA (2000) Geostatistics for environmental scientists. Wiley & Sons, Ltd., UK

Zhou ZY, Sun OJ, Luo ZK, Jin HM, Chen QS, Han XG (2008) Variation in small-scale spatial heterogeneity of soil properties and vegetation with different land use in semiarid grassland ecosystem. Plant Soil 310:103–112 doi:10.1007/s11104-008-9633-1